Subscriber access provided by American Chemical Society

Article

Infrared Spectra of CH–MoH, CHMoH, and CH#MoH Formed by Activation of CH by Molybdenum Atoms

Han-Gook Cho, and Lester Andrews

J. Am. Chem. Soc., **2005**, 127 (22), 8226-8231• DOI: 10.1021/ja0511568 • Publication Date (Web): 14 May 2005

Downloaded from http://pubs.acs.org on March 25, 2009

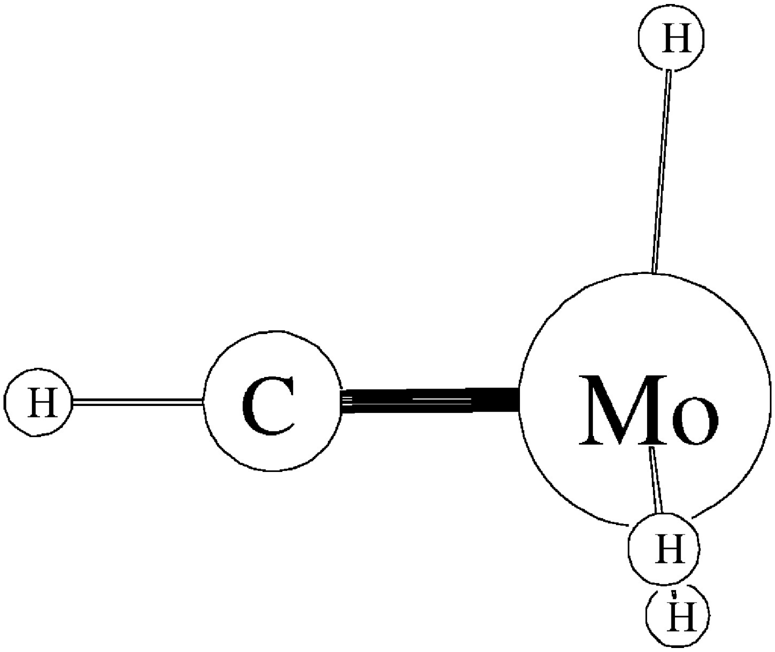

More About This Article

Additional resources and features associated with this article are available within the HTML version:

- Supporting Information
- Links to the 11 articles that cite this article, as of the time of this article download
- Access to high resolution figures
- Links to articles and content related to this article
- Copyright permission to reproduce figures and/or text from this article

View the Full Text HTML

High quality. High impact.

Journal of the American Chemical Society is published by the American Chemical Society. 1155 Sixteenth Street N.W., Washington, DC 20036

J|A|C|S
A R T I C L E S
Published on Web 05/14/2005

Infrared Spectra of CH_3-MoH, $CH_2=MoH_2$, and $CH\equiv MoH_3$ Formed by Activation of CH_4 by Molybdenum Atoms

Han-Gook Cho and Lester Andrews*

Contribution from the Department of Chemistry, University of Incheon, 177 Dohwa-dong, Nam-ku, Incheon, 402-749, South Korea, and the Department of Chemistry, University of Virginia, P.O. Box 400319, Charlottesville, Virginia 22904-4319

Received February 23, 2005; E-mail: lsa@virginia.edu

Abstract: Reaction of laser-ablated Mo atoms with CH_4 in excess argon forms the CH_3-MoH, $CH_2=MoH_2$, and $CH\equiv MoH_3$ molecules, which are identified from infrared spectra by isotopic substitution and density functional theory frequency calculations. These simple methyl, methylidene, and methylidyne molybdenum hydride molecules are reversibly interconverted by α-H transfers upon visible and ultraviolet irradiations. The methylidene dihydride $CH_2=MoH_2$ exhibits CH_2 and MoH_2 distortion and agostic interaction to a lesser degree than $CH_2=ZrH_2$. Molybdenum methylidyne trihydride $CH\equiv MoH_3$ is a stable C_{3v} symmetry molecule.

Introduction

The early transition metals in group 4 activate methane to form simple methylidene dihydrides, $CH_2=MH_2$, which exhibit the effects of agostic bonding.[1-3] Density functional calculations using large basis sets show that the two metal hydride bond lengths are different and that the CH_2 subunit is distorted with H−C−M angles of 91.6°, 92.9°, and 95.6° for M = Ti, Zr, and Hf, respectively.[4-7] Earlier computations using minimum basis sets failed to find this agostic distortion.[8-10] Polarization functions in the electronic structure calculation are necessary to characterize the agostic interaction.[1,5] The analogous methylidene complexes prepared from methyl fluoride, $CH_2=MHF$, showed the same trend in agostic bonding.[11-13] High oxidation state transition metal alkylidene complexes ($R_1R_2C=M$) are common in organometallic chemistry where bulky substituents are required to stabilize the electron-deficient metal center, and many of these compounds are agostic.[14] These complexes play important roles in alkane activation and alkene metathesis reactions.[14-16] In addition, the alkylidene complexes of group 6 can rearrange into the analogous alkylidyne complexes ($RC\equiv M$), and a number of $R-C\equiv MoX_3$ complexes have been prepared.[14] The molybdenum methylidyne complex $HC\equiv Mo(N(t\text{-}Bu)Ar)_3$ has recently been synthesized.[17] Accordingly, we have investigated Mo atom reactions with methane to explore further agostic bonding in simple $CH_2=MH_2$ methylidene hydride complexes and to initiate α-H transfer to form the first example of the simplest methylidyne hydride complex $HC\equiv MoH_3$. Our electronic structure calculations show that this molecule has C_{3v} symmetry, and $HC\equiv MoH_3$ is characterized here by matrix infrared spectroscopy.

Experimental and Computational Methods

The laser-ablation matrix infrared experiment has been described previously.[18-20] Briefly, laser-ablated molybdenum atoms (Goodfellow) were reacted with CH_4 (Matheson, UHP grade), $^{13}CH_4$, CD_4, and CH_2D_2 (Cambridge Isotopic Laboratories) in excess argon (MG Industries) during condensation on a CsI window at 8 K. Infrared spectra were recorded at 0.5 cm^{-1} resolution on a Nicolet 550 spectrometer with type B liquid nitrogen-cooled HgCdTe detector. Samples were irradiated by a mercury arc lamp (175 W, globe removed) for 20 min periods and were annealed, and more spectra were recorded.

Complementary density functional theory (DFT) calculations were done using the Gaussian 98 package,[21] B3LYP density functional, the large 6-311++G(3df, 3pd) basis set for C and H, and the SDD effective core potential and basis set for Mo (14 valence electrons) to provide a consistent set of vibrational frequencies for anticipated reaction products. Geometries were fully relaxed during optimization, and the optimized geometry was confirmed through vibrational analysis. All the vibrational frequencies were calculated analytically.

---

(1) Ujaque, G.; Cooper, A. C.; Maseras, F.; Eisenstein, O.; Caulton, K. G. *J. Am. Chem. Soc.* **1998**, *120*, 361.
(2) (a) Eisenstein, O.; Jean, Y. *J. Am. Chem. Soc.* **1985**, *107*, 1177. (b) Clot, E.; Eisenstein, O. Agostic Interactions from a Computational Perspective. In *Structure and Bonding, Computational Inorganic Chemistry*, Kaltzoyannis, N., McGrady, J. E., Eds.; Springer-Verlag: Heidelberg, 2004; pp 1−36.
(3) Scherer, W.; McGrady, G. S. *Angew. Chem., Int. Ed.* **2004**, *43*, 1782.
(4) Andrews, L.; Cho, H.-G.; Wang, X. *Angew. Chem.* **2005**, *117*, 115.
(5) Cho, H.-G.; Wang, X.; Andrews, L. *J. Am. Chem. Soc.* **2005**, *127*, 465.
(6) Andrews, L.; Cho, H.-G.; Wang, X. *Inorg. Chem.* **2005**, in press (Ti+CH_4).
(7) Cho, H.-G.; Wang, X.; Andrews, L. *Organometallics* **2005**, *24*, 2854−2861.
(8) Franci, M. M.; Pietro, W. J.; Hout, R. F., Jr.; Hehre, W. J. *Organometallics* **1983**, *2*, 281.
(9) Franci, M. M.; Pietro, W. J.; Hout, R. F., Jr.; Hehre, W. J. *Organometallics* **1983**, *2*, 815.
(10) Cundari, T. R.; Gordon, M. S. *J. Am. Chem. Soc*. **1992**, *114*, 539.
(11) Cho, H.-G.; Andrews, L. *J. Phys. Chem. A* **2004**, *108*, 6294.
(12) Cho, H.-G.; Andrews, L. *J. Am. Chem. Soc.* **2004**, *126*, 10485.
(13) Cho, H.-G.; Andrews, L. *Organometallics* **2004**, *23*, 4357.
(14) Schrock, R. R. *Chem. Rev.* **2002**, *102*, 145.
(15) Buchmeiser, M. R. *Chem. Rev.* **2000**, *100*, 1565.
(16) Crabtree, R. H. *Chem. Rev.* **1985**, *85*, 245.
(17) Agapie, T.; Diaconescu, P. L.; Cummins, C. C. *J. Am. Chem. Soc.* **2002**, *124*, 2412.
(18) Andrews, L.; Citra, A. *Chem. Rev.* **2002**, *102*, 885, and references therein.
(19) Andrews, L.; Wang, X. *J. Am. Chem. Soc.* **2003**, *125*, 11751.
(20) Wang, X.; Andrews, L. *J. Phys. Chem. A* **2003**, *107*, 570.
(21) Frisch, M. J.; et al. *Gaussian 98*, Revision A.11.4; Gaussian, Inc.: Pittsburgh, PA, 2002.

10.1021/ja0511568 CCC: $30.25 © 2005 American Chemical Society

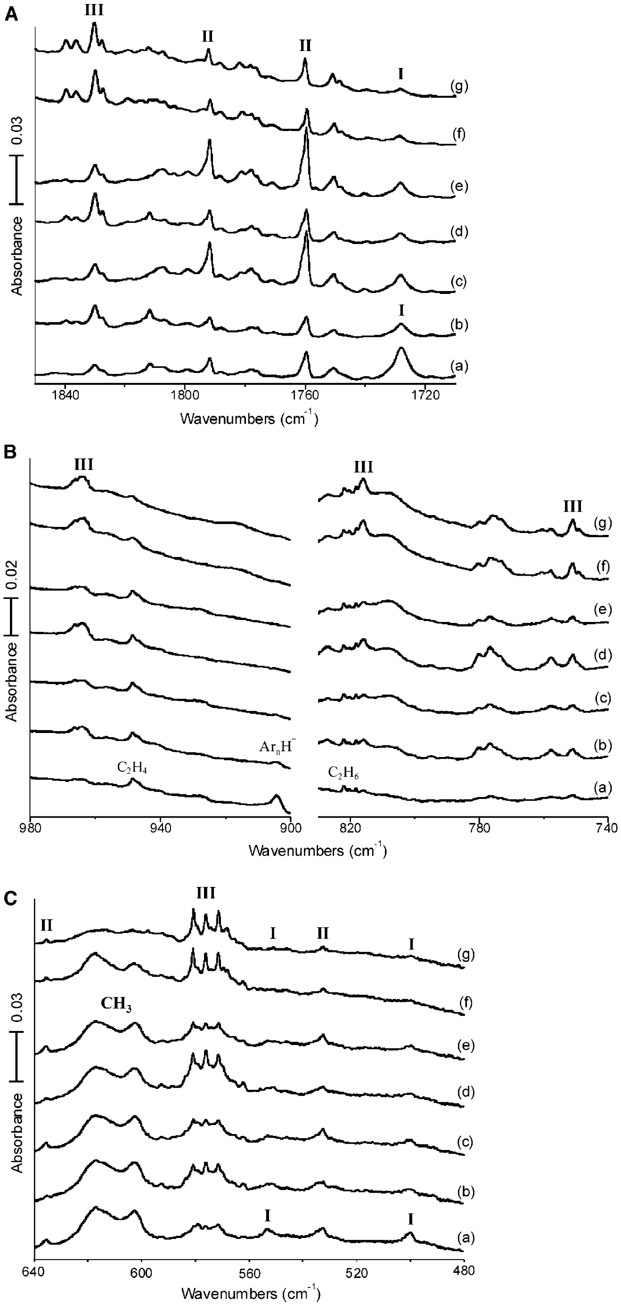

Figure 1. Infrared spectra for laser-ablated Mo co-deposited with CH_4 in excess argon at 8 K. (a) Mo and 2% CH_4 in argon deposited for 60 min, (b) after $\lambda > 420$ nm irradiation for 20 min, (c) after 240−380 nm irradiation, (d) after $\lambda > 420$ nm irradiation for 20 min, (e) after 240−380 nm irradiation, (f) after $\lambda > 420$ nm irradiation for 20 min, and (g) after annealing to 26 K.

Results

The products of the activation of methane by molybdenum atoms will be characterized by matrix infrared spectroscopy and electronic structure calculations.

Table 1. Infrared Absorptions (cm^{-1}) Observed for Laser-Ablated Mo Atom and Methane Reaction Products in Excess Argon

CH_4	$^{13}CH_4$	CD_4	CH_2D_2	identity[a]
1839.7	1839.7	1329.3		III (CH_4)
1836.4	1836.4			III (CH_4)
1830.0	1830.0	1320.7	1829.3, 1326.4	III
1811.8	1811.8	1312.6		X
1807.5	1807.5	1307.8		X′
1791.6	1791.6	1287.4	1791.6, 1286.9	II
1781.5	1781.5	1281.8	1779.5, 1772.0 1280.0, 1273.3	II (CH_4)
1759.6	1759.6	1264.9	1759.6, 1264.9	II
1750.6	1750.6	1258.2		II (CH_4)
1728.0	1728.0	1240.4	1728.0	I
964.0	934.9	918.5	964.5, 916.0	III
904.2	904.2	643.8	904.2, 643.5	Ar_nH^+, Ar_nD^+
816.1	815.2	593.9	768.7, 644.4	III
776.7	776.0	559.1		?
751.2	747.3	554.9		III
635.4	631.3			II
617, 603	612, 598	453		CH_3, CD_3
			495.0	I
580.8	580.4			III
576.2	575.9			III
571.5	571.1			III
553.6	551.0			I
532.5	532.2			II
500.3	487.2			I

[a] I denotes $CH_3{-}MoH$, II indicates $CH_2{=}MoH_2$, and III identifies $CH{\equiv}MoH_3$.

Infrared Spectra. Laser-ablated Mo atoms and CH_4 were reacted and product photochemistry was explored in several experiments. Figure 1 illustrates infrared spectra using 2% CH_4 in argon. Three major groups of product absorptions are characterized by their distinct photochemistry. Starting with the Mo−H stretching region, new absorptions are observed at 1728.0 (labeled I), 1791.6 (labeled II), 1759.6 (labeled II), and 1830.0 cm^{-1} (labeled III) on sample deposition. Irradiation with visible light ($\lambda > 420$ nm) decreased I and II and increased III, and ultraviolet irradiation (240−380 nm) decreased III while markedly increasing II and slightly increasing I. This visible and ultraviolet irradiation sequence was repeated (Figure 1d−f) with the same result, and the photochemical processes appear to be reversible. A final annealing to 26 K had little effect on the spectrum. Other absorptions showed the same photochemical behavior, and these are illustrated for the lower frequency regions. The observed absorptions are listed in Table 1, where they are identified by parallel photochemical behavior as I, II, or III, respectively. Bands also identified with (CH_4) are probably due to methane complexes with that product. Owing to photochemistry from the ablation plume, absorptions were observed for the CH_3 radical, the matrix-solvated proton, C_2H_2, C_2H_4, and C_2H_6.[22−27]

Similar experiments were done with methane reagents modified by isotopic substitution. In the upper region $^{13}CH_4$ gave the same unshifted product bands, and in the lower region these bands shifted slightly, but they exhibited the same photochemistry as the $^{12}CH_4$ counterparts. All bands shifted with CD_4, as shown in Figure 2 and listed in Table 1, and photochemistry facilitated grouping with the I, II, and III product species. The CH_2D_2 precursor yielded product bands involving both H and D vibrations, which are of considerable diagnostic value. Arrows indicate new mixed H, D product absorptions from the CH_2D_2 precursor in Figure 3.

Calculations. Density functional theory computations were done for the anticipated $CH_3{-}MoH$ and $CH_2{=}MoH_2$ products.

---

(22) Jacox, M. E. *J. Mol. Spectrosc.* **1977**, *66*, 272.
(23) Milligan, D. E.; Jacox, M. E. *J. Mol. Spectrosc.* **1973**, *46*, 460.
(24) Wight, C. A.; Ault, B. S.; Andrews, L. *J. Chem. Phys.* **1976**, *65*, 1244.
(25) Wang, X.; Andrews, L. *J. Phys. Chem. A* **2003**, *107*, 337.
(26) Cho, H.-G.; Andrews, L. *J. Phys. Chem. A* **2004**, *108*, 3965
(27) Davis, S. R.; Andrews, L. *J. Am. Chem. Soc.* **1987**, *109*, 4768.

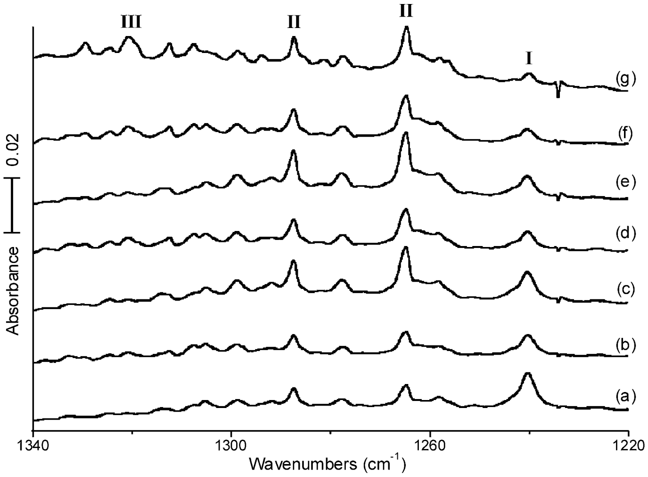

Figure 2. Infrared spectra in the 1340−1220 cm^{-1} region for laser-ablated Mo co-deposited with CD_4 in excess argon at 8 K. (a) Mo and 2% CD_4 in argon deposited for 60 min, (b) after $\lambda > 420$ nm irradiation for 20 min, (c) after 240−380 nm irradiation, (d) after $\lambda > 420$ nm irradiation for 20 min, (e) after 240−380 nm irradiation, (f) after $\lambda > 420$ nm irradiation for 20 min, and (g) after annealing to 26 K.

In agreement with Bloomberg et al.,[28] we find a $^5A'$ ground state for CH_3−MoH, and the structure computed with the B3LYP density functional, large 6-311++G(3df, 3pd) basis set, and SDD pseudopotential and basis for Mo is given in Figure 4. A triplet state with almost the same structure is 20 kcal/mol higher in energy, which is displayed in Figure 5. Next, we calculate low-energy triplet states for CH_2=MoH_2 and find a planar, symmetrical (C_{2v}) structure 0.4 kcal/mol lower than a nonplanar, distorted (C_1) structure. The nonplanar $^3A''$ structure shown in Figure 4 has less agostic CH_2 distortion than found for CH_2=ZrH_2 and computed frequencies that match the experimental spectrum much better than those for the almost isoergic planar structure. (The BPW91 density functional gives almost the same planar and nonplanar structures separated by 0.3 kcal/mol.) The nonplanar CH_2=MoH_2 species is 12 kcal/mol higher in energy than CH_3−MoH. We found a nonagostic quintet state CH_2−MoH_2 (C−Mo, 2.058 Å) with equivalent C−H and Mo−H bonds to be 6 kcal/mol higher in energy and an almost C_{2v} singlet state CH_2=MoH_2 (C=Mo, 1.859 Å) to be 21 kcal/mol higher in energy than the ground triplet state for CH_2=MoH_2, which are compared in Figure 5. Higher level calculations will be required for a more accurate description of triplet CH_2=MoH_2.

In this regard, the CH_2=MoH_2 calculations were repeated using SDD+f for Mo, and the structure and frequencies were almost the same (H′−C−Mo, 115.4°; C=Mo, 1.861 Å; H′−C, 1.099 Å; 1891.3, 1854.9, 656.2 cm^{-1}) and the Mulliken charges showed slightly less polarity (C, −0.67; Mo, 1.22).

In contrast to Zr, a stable hexavalent CH≡MoH_3 species was calculated, with a singlet ground state ($^1A_1$) in C_{3v} symmetry, which is 11 kcal/mol higher in energy than CH_3−MoH. We located a $^3A'$ state CH=MoH_3 (C=Mo, 1.819 Å and angle H−C=Mo, 174.0°) in C_s symmetry to be 36 kcal/mol higher in energy than the ground state. This excited state has 1815, 1819, and 1975 cm^{-1} Mo−H stretching frequencies and 1.725, 1.725, and 1.672 Å Mo−H bond lengths.

Isotopic vibrational frequencies computed for these structures in the harmonic approximation are helpful for assignment of the new infrared absorptions observed here to Mo and CH_4 reaction products with carbon−molybdenum bonds. Tables 2 and 3 collect computed frequencies for the new methylidene and methylidyne species, and Table 4 lists Mulliken charges and natural valence electron configurations computed for the product molecules. Figure 5 summarizes the relative energies of the lowest electronic states found for CH_3MoH, CH_2MoH_2, and $CHMoH_3$.

Following the example of $(CH_3)_2ZrH_2$, we computed a stable triplet state $(CH_3)_2MoH_2$ molecule, which has almost the same structure as the Zr counterpart,[4,5] and Mo−H_2 stretching frequencies at 1876.9 cm^{-1} (271 km/mol) and 1901.0 cm^{-1} (184 km/mol) using the 6-311++G(2d, p) basis set.

Discussion

The three groups of product absorptions will be assigned on the basis of photochemistry, isotopic substitution, and comparison with DFT calculations.

CH_3−MoH. The strongest absorption computed for CH_3−MoH is the Mo−H stretching mode, 1813.3 cm^{-1} (234 km/mol intensity). The strongest initial I product absorption at 1728.0 cm^{-1} is assigned accordingly. The lack of ^{13}C shift and deuterium counterpart at 1240.4 cm^{-1} (H/D ratio 1.3931) support this assignment. This band is unshifted for CHD_2−MoH formed in the CH_2D_2 experiments. Other absorptions that might be observable are computed at 622.6 cm^{-1} (52 km/mol, CH_3 rock + Mo−H bend), 568.5 cm^{-1} (21 km/mol, CH_3 wag), and 499.6 cm^{-1} (17 km/mol, C−Mo stretch). The former is masked by strong CH_3 absorption, but the CD_3MoD counterpart is observed at 495.0 cm^{-1}. The latter modes are produced in solid argon at 553.6 and 500.3 cm^{-1} (Figure 1). The observed ^{13}C shifts (2.6 and 13.1 cm^{-1}, respectively) are in excellent agreement with the calculated (2.8 and 12.9 cm^{-1}) values. This agreement between calculated and observed frequencies for four different fundamentals confirms the assignments to CH_3−MoH, particularly with the diagnostic single-bond C−Mo stretching mode at 500.3 cm^{-1}.

CH_2=MoH_2. The two strong II absorptions at 1791.6 and 1759.6 cm^{-1} are characterized by identical band profiles and photochemical behavior in six successive spectra (Figure 1). The strongest absorptions for CH_2=MoH_2 are calculated (Table 2) for the nonplanar structure at 1890.2 cm^{-1} (symmetric in-phase Mo−H_2, mostly shorter out-of-plane Mo−H bond stretch) and at 1854.9 cm^{-1} (antisymmetric out-of-phase Mo−H_2, mostly longer in-plane Mo−H bond stretch), and the above II absorptions are assigned accordingly. This calculated 35.3 cm^{-1} Mo−H stretching mode separation is in very good agreement with the 32.0 cm^{-1} experimental value. The observed H/D ratios, 1.3916 and 1.3931, are appropriate, and the scale factors (observed/calculated, 0.948 and 0.949) are almost the same as the 0.953 value determined here for CH_3−MoH and values for other transition metal compounds.[29] Additional group II absorptions are observed at 635.4 and 532.5 cm^{-1}. Computed frequencies at 647.0 and 530.5 cm^{-1} for MoH_2 bend and wag modes with 2.1 and 0.1 cm^{-1} ^{13}C shifts are in very good agreement with the observed values (Table 1). Hence, nonplanar CH_2=MoH_2

---

(28) Bloomberg, M. R. A.; Siegbahn, P. E. M.; Swensson, M. *J. Am. Chem. Soc.* **1992**, *114*, 6095.

(29) Bytheway, I.; Wong, M. W. *Chem. Phys. Lett.* **1998**, *282*, 219.

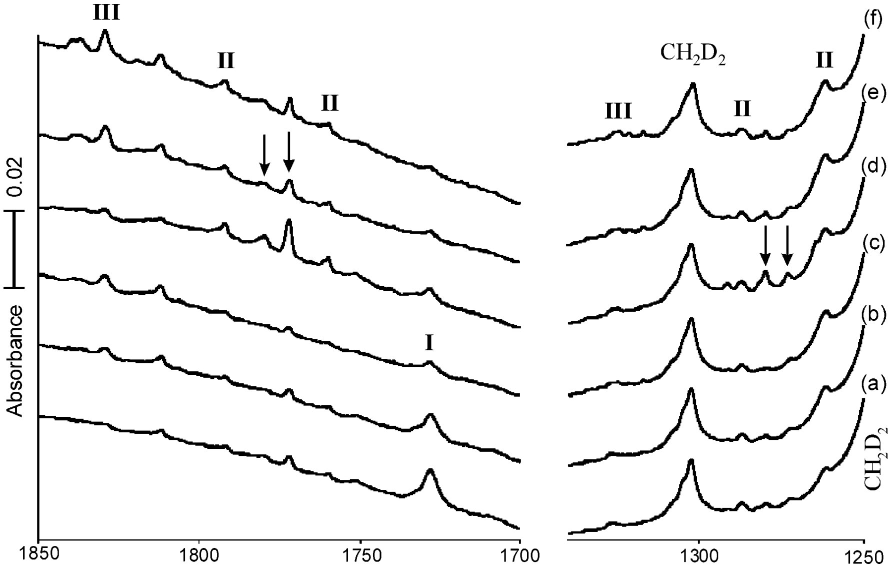

Figure 3. Infrared spectra in the 1850−1700 and 1340−1250 cm^{-1} regions for laser-ablated Mo co-deposited with CH_2D_2 in excess argon at 8 K. (a) Mo and 2% CH_2D_2 in argon deposited for 60 min, (b) after $\lambda > 530$ nm irradiation for 20 min, (c) after 420 nm irradiation, (d) after 240−380 nm irradiation, (e) after $\lambda > 420$ nm irradiation for 20 min, and (f) after annealing to 26 K.

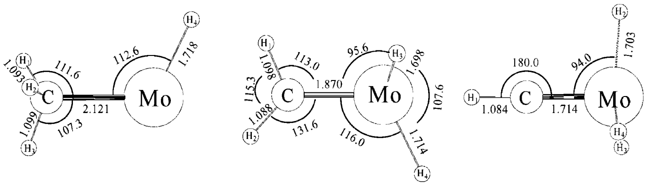

CH_3-MoH ($^5A'$) CH_2=MoH_2 ($^3A''$) CH≡MoH_3 ($^1A'$)

Figure 4. Structures computed for CH_3−MoH ($^5A'$), CH_2=MoH_2 ($^3A''$), and CH≡MoH_3 ($^1A'$) at the B3LYP/6-311++G(3df, 3pd)/SDD level of theory. Bond distances, angstroms, and bond angles, degrees.

is here identified by appropriate agreement between observed and calculated isotopic frequencies for four fundamental vibrations.

The corresponding frequencies computed for the symmetrical planar structure do not fit the observed frequencies: First, the calculated MoH_2 stretching mode separation (4.3 cm^{-1}) is much less than the 32.0 cm^{-1} observed separation. Second, the computed MoH_2 bend is 60 cm^{-1} higher (9.4%) than the observed mode, and third, the MoH_2 wag is predicted with no intensity for this observed absorption. Finally, Mo−H and Mo−D stretching modes for CHD=MoHD are predicted at the average Mo−H_2 and the average Mo−D_2 positions, and two such bands are observed *both above and below the averages*, which demonstrates nonequivalent Mo−H bonds and rules out a symmetrical structure.

The inequivalent CH_2 and MoH_2 bonds are manifest in the CH_2D_2 experiments as four different mixed CHD=MoHD isomers are possible (see Chart 1 in ref 5 for isotopomers 3, 4, 5, and 6). In fact new absorptions are observed at 1779.5 and 1772.0 cm^{-1} (marked by arrows) between the two Mo−H_2 stretching modes for CD_2=MoH_2 at 1791.6 and 1759.6 cm^{-1} (labeled II) and at 1280.0 and 1273.3 cm^{-1} (marked by arrows) between the two Mo−D_2 stretching modes for CH_2=MoD_2 at 1286.9 and 1264.9 cm^{-1} (labeled II) (Figure 3). Isotopomers 4 and 6 with H in the shorter bond out-of-plane position are computed to be 32.6 cm^{-1} higher for Mo−H and 1.4 cm^{-1} for Mo−D from the stronger frequencies observed for CD_2=MoH_2 and CH_2=MoD_2, respectively, for the distorted structure in Figure 4, and our observed new bands are 20.4 and 8.4 cm^{-1} higher. Isotopomers 3 and 5 with D in the shorter bond out-of-plane position are calculated to be 2.9 cm^{-1} higher for Mo−H and 23.0 cm^{-1} for Mo−D, and our new bands are 15.1 and 12.3 cm^{-1} higher. This agreement is not as good as found for singlet CH_2=ZrH_2.[5] Triplet CH_2=MoH_2 is a more difficult subject for theory, and our computation predicts slightly more inequivalence and less coupling between the two Mo−H bonds than is manifest in the vibrational spectra. This depends on the

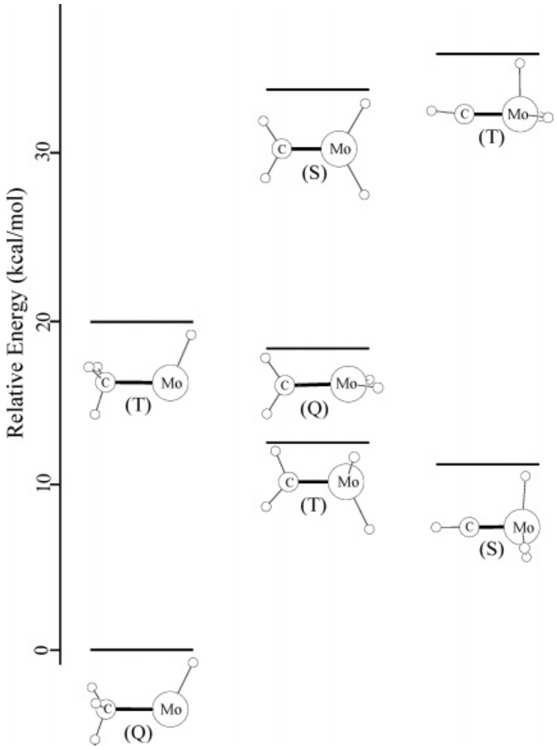

Figure 5. Relative energies of the lowest energy CH_3MoH, CH_2MoH_2, and $CHMoH_3$ electronic states that are involved in the reversible α-H transfer photochemistry. Q denotes quintet, T indicates triplet, and S denotes singlet electronic states.

Table 2. Harmonic Vibrational Frequencies (cm^{-1}) Computed[a] for the Nonplanar ($^3A''$) Triplet Ground State Structure of $CH_2{=}MoH_2$

mode description	$^{12}CH_2{=}MoH_2$ freq[b]	int[c]	$^{13}CH_2{=}MoH_2$ freq[b]	$CD_2{=}MoD_2$ freq[b]	int[c]
CH_2 str	3145.0	(1)	3133.6	2331.4	(0)
CH_2 str	2998.1	(1)	2992.2	2174.7	(0)
MoH_2 str[d]	1890.2	(148)	1890.2	1343.5	(79)
MoH_2 str[d]	1854.9	(301)	1854.9	1320.1	(153)
CH_2 scis	1326.3	(2)	1316.7	1041.7	(4)
CH_2 wag	775.7	(33)	768.3	652.8	(26)
C═Mo str	742.4	(53)	725.6	614.5	(26)
MoH_2 bend[d]	647.0	(105)	644.9	474.2	(21)
MoH_2 rock	616.9	(5)	613.2	457.9	(4)
MoH_2 wag[d]	530.5	(36)	530.4	379.4	(17)
CH_2 rock	301.6	(19)	301.0	217.3	(11)
CH_2 twist	221.8	(44)	221.7	158.2	(22)

[a] B3LYP/6-311++G(3df, 3pd)/SDD. [b] Frequencies, cm^{-1}. [c] Intensities, km/mol. [d] Corresponding frequencies for planar structure: 1842.1 (199), 1837.9 (316), 695.0 (92), and 545.5 (0).

Table 3. Harmonic Vibrational Frequencies Computed[a] for the $^1A_1$ Ground Singlet State C_{3v} Structure of $CH{\equiv}MoH_3$

mode description	$^{12}CH{\equiv}MoH_3$ freq[b] (int)[c]	$^{13}CH{\equiv}MoH_3$ freq[b]	$CD{\equiv}MoD_3$ freq[b] (int)[c]
C−H str	3205.7 (11)	3194.0	2383.5 (11)
Mo−H str	1911.5 (274 × 2)	1911.5	1364.3 (142 × 2)
Mo−H str	1911.2 (90)	1911.2	1352.4 (44)
C≡Mo str	1055.5 (23)	1022.8	1007.7 (19)
$Mo{-}H_2$ bend	860.2 (40 × 2)	59.6	638.0 (0.1 × 2)
Mo≡C−H bend	791.6 (12 × 2)	784.4	604.3 (26 × 2)
sym MoH_3 def	638.0 (56)	637.6	457.4 (29)
MoH_3 rock	573.0 (77 × 2)	573.0	406.5 (39 × 2)

[a] B3LYP/6-311++G(3df, 3pd)/SDD. [b] Frequencies, cm^{-1}. [c] Intensities, km/mol. Double intensities are for e modes, others are a_1 modes.

Table 4. Mulliken Charges and Natural Valence Electron Configurations Calculated[a] for C, H, and Mo Species in Figure 4

atom	$CH_3{-}MoH$	$CH_2{=}MoH_2$	$CH{\equiv}MoH_3$
C	-0.85 ($2s^{1.22}2p^{3.73}$)[b]	-0.71 ($2s^{1.24}2p^{3.37}$)	-0.66 ($2s^{1.28}2p^{2.90}$)
H_1	+0.065 ($1s^{0.80}$)	+0.036 ($1s^{0.81}$)	+0.06 ($1s^{0.83}$)
H_2	+0.065 ($1s^{0.80}$)	+0.038 ($1s^{0.82}$)	-0.28 ($1s^{1.14}$)
Mo	+0.97 ($5s^{0.66}5d^{4.67}$)	+1.26 ($5s^{0.58}5d^{4.75}$)	+1.45 ($5s^{0.60}5d^{4.99}$)
H_3	+0.07 ($1s^{0.81}$)	-0.34 ($1s^{1.23}$)	-0.28 ($1s^{1.14}$)
H_4	-0.32 ($1s^{1.29}$)	-0.28 ($1s^{1.18}$)	-0.28 ($1s^{1.14}$)

[a] B3LYP/6-311++G(3df, 3pd)/SDD. [b] Natural valence electron configurations.

H−Mo−H angle, which is very sensitive to the theoretical methods employed. The observation of two mixed CHD═MoHD absorptions in each region (Figure 3) confirms the inequivalent Mo−H bonds computed for the agostic $CH_2{=}MoH_2$ structure (Figure 4).

The $Mo{-}H_2$ stretching frequencies for $CH_2{=}MoH_2$ may be compared to those observed for MoH_2. Xiao et al. assigned the strongest MoH_2 band as 1727.4 cm^{-1} in solid argon at 12 K,[30] and we observe this band at 1718.8 cm^{-1} using laser-ablated Mo atoms and H_2 reagent in solid argon at 5 K.[31] In either case the MoH_2 stretching frequencies of $CH_2{=}MoH_2$ are slightly higher. It is important to note that none of the present $Mo{+}CH_4$ reaction product frequencies are observed in the $Mo{+}H_2$ reaction system, which shows that binary MoH_x species are not produced in the methane experiments.

The simple methylidene dihydride complex $CH_2{=}MoH_2$ we have characterized in solid argon has a DFT-computed 1.870 Å C═Mo double-bond length. This bond length may be compared with X-ray diffraction values ranging from 1.827 to 1.878 Å for several heavily ligated and substituted methylidene complexes reviewed by Schrock.[14]

Even though the C═Mo bond is computed to be shorter than the C═Zr bond in the corresponding $CH_2{=}MH_2$ methylidene,[5] the agostic distortion for the CH_2 group (H−C−M angle, 92.9°) is much greater for the Zr than the Mo methylidene dihydride (113.0°). Computed Mulliken charges are also larger for the Zr compound, and the C═M and M−H bonds are more polar. We suggest that the extra 4d electrons in triplet $CH_2{=}MoH_2$ diminish the agostic interaction relative to that for $CH_2{=}ZrH_2$. This is substantiated by d orbital populations, as all d orbitals on Mo are occupied (0.93 to 0.99 with total 4.75), which therefore reduces the agostic interaction. (The total d occupation is 2.08 for Zr in $CH_2{=}ZrH_2$.)[7] It appears that less CH_2 distortion is required to stabilize $CH_2{=}MoH_2$ because the metal hydride bonds distort more in relative length and orientation in order to stabilize the C═M double bond, which is a consequence of the agostic interaction.[1−3]

$CH{\equiv}MoH_3$. The highest frequency new product absorption observed at 1830.0 cm^{-1} is formed by visible photodestruction of $CH_3{-}MoH$ and $CH_2{=}MoH_2$, and it does not increase spontaneously on annealing, in contrast to the $(CH_3)_2ZrH_2$ secondary reaction product.[5] The 1830.0 cm^{-1} absorption defines the 1830.0/1320.7 = 1.3856 H/D ratio for an Mo−H stretching mode, but the CH_2D_2 precursor gives 1829.3 and 1326.4 cm^{-1} absorptions, which demonstrate slight coupling with adjacent H(D) atoms. Computations for the possible $CH{\equiv}MoH_3$ methylidyne product predict very strong antisymmetric and symmetric Mo−H stretching modes at 1911.5 and 1911.2 cm^{-1}, which are higher than the Mo−H stretching modes for $CH_2{=}MoH_2$, and the scale factor 1830.0/1911.5 = 0.957 is in line with observations for the above species. The higher frequency 1830.0 cm^{-1} absorption is thus assigned to both overlapped Mo−H stretching modes for $CH{\equiv}MoH_3$. The other bands are due to matrix site splittings or aggregation with unreacted methane. The weak 1811.8 cm^{-1} band exhibits still different photochemistry, and this single absorption is due to an unidentified Mo−H species.

Our preparation of $CH{\equiv}MoH_3$ is confirmed by the observation of four other strong modes that correlate with those predicted by DFT computations. The C≡Mo stretching mode is calculated at 1055.5 cm^{-1} with 32.8 and 47.8 cm^{-1} ^{13}C and D shifts and observed at 964.0 cm^{-1} with 29.1 and 45.5 cm^{-1} isotopic shifts, respectively. The degenerate $Mo{-}H_2$ valence angle bending mode is predicted at 860.2 cm^{-1} with 0.6 and 222.2 cm^{-1} ^{13}C and D shifts and observed at 816.1 cm^{-1} with 0.9 and 222.2 cm^{-1} isotopic shifts, respectively. The degenerate Mo≡C−H bending mode is computed at 791.6 cm^{-1} with 7.2 and 187.3 cm^{-1} ^{13}C and D shifts and observed at 751.2 cm^{-1} with 3.9 and 196.3 cm^{-1} isotopic shifts, respectively. Scale factors (0.91, 0.95, 0.95) are required to match the above calculated and observed frequencies. The degenerate MoH_3 deformation is predicted at 573.0 cm^{-1} with no ^{13}C shift and D shift below our limit of detection. We observe this band split by the matrix into three sharp bands at 580.8, 576.2, and 571.5 cm^{-1} with 0.3−0.4 cm^{-1} ^{13}C shifts. The close matching of five

---

(30) Xiao, Z. L.; Hauge, R. H.; Margrave, J. L. *J. Phys. Chem.* **1992**, *96*, 636 ($Mo{+}H_2$).
(31) Wang, X.; Andrews, L. Unpublished results, 2003.

Scheme 1

$$\mathrm{Mo}\,(^7\mathrm{S}) + \mathrm{CH_4} \xrightarrow{\mathrm{UV}} \mathrm{CH_3{-}MoH} \underset{\mathrm{UV}}{\overset{\mathrm{VIS}}{\rightleftarrows}} \mathrm{CH_2{=}MoH_2} \underset{\mathrm{UV}}{\overset{\mathrm{VIS}}{\rightleftarrows}} \mathrm{CH{\equiv}MoH_3}$$

strong calculated and observed vibrational fundamentals and isotopic fundamentals for ^{13}C and D substitution substantiates our observation and characterization of the first simple transition metal methylidyne trihydride complex, $CH{\equiv}MoH_3$. This novel molecule is computed to have C_{3v} symmetry in the singlet ground state.

The C≡Mo triple bond length computed here for the simple $CH{\equiv}MoH_3$ compound, 1.714 Å, is slightly shorter than the 1.743 and 1.754 Å values measured for $(AdO)_3Mo{\equiv}CR$ complexes[14,32] and the 1.762 Å triple bond length recently determined for $(R_1R_2N)_3Mo{\equiv}CPPh^-$.[17] The successful DFT calculation of a 1.777 Å triple bond length in the $(H_2N)_3$-$Mo{\equiv}CPPh^-$ model compound[17] supports our DFT results on the simple $HC{\equiv}MoH_3$ molecule.

We note the substantial increase in Mulliken charge on Mo in the series $CH_3{-}MoH$, $CH_2{=}MoH_2$, and $CH{\equiv}MoH_3$ (Table 4) with additional hydrides bonded to Mo. This additional charge on the Mo center contracts the 4d orbitals and facilitates the formation of multiple bonds to carbon in the series with increasing metal oxidation state, which is shown by the corresponding increase in d orbital populations.

Reaction Mechanisms. Laser-ablated Mo atoms are sufficiently excited to overcome the activation energy[28] required for C−H insertion to form $CH_3{-}MoH$. Smaller amounts of $CH_2{=}MoH_2$ and $CH{\equiv}MoH_3$ result from successive α-H transfers[33] in the energized $[CH_3MoH]^*$ and $[CH_2MoH_2]^*$ intermediates so formed. Next we employ photochemistry to group the three major product absorptions from the activation of methane by molybdenum atoms, Scheme 1. Visible irradiation of the initial $CH_3{-}MoH$ formed on reaction with excited laser-ablated Mo atoms markedly decreases I, slightly decreases II, and substantially increases III. Thus, by two successive α-H transfers $CH_3{-}MoH$ rearranges to $CH_2{=}MoH_2$ and to $CH{\equiv}MoH_3$. Subsequent ultraviolet irradiation reverses the process, but $CH_2{=}MoH_2$ is favored over lower energy $CH_3{-}MoH$ since one hydrogen on Mo is restored to carbon more rapidly than two. The infrared spectra in Figure 1 clearly show that these successive α-H transfers are completely reversible. Finally, 240−380 nm irradiation contains the $^7S \rightarrow {}^7P$ resonance absorption of Mo in solid argon,[35] and this excitation can promote the insertion reaction to form $CH_3{-}MoH$.

Figure 5 displays the relative energies of the low lying electronic states of CH_3MoH, CH_2MoH_2, and $CHMoH_3$ that are involved in the photochemistry. Our B3LYP calculations find $CH_3{-}MoH$ the lowest in energy of the three products: The ground state methylidene is computed to be 12 kcal/mol higher in energy, and the methylidyne only 11 kcal/mol higher than $CH_3{-}MoH$. Upon visible irradiation $CH_3{-}MoH$ (Q) is excited to a higher quintet state and α-H transfers to form $CH_2{-}MoH_2$ (Q),[34] which then relaxes in the matrix to the ground state $CH_2{=}MoH_2$ (T) with agostic bonding. The latter is also excited to a higher triplet state and α-H transfers to give $CH{=}MoH_3$ (T), which is subsequently de-energized by the matrix to stabilize the final $CH{\equiv}MoH_3$ (S) product. Upon near-ultraviolet irradiation $CH{\equiv}MoH_3$ (S) is excited to a higher singlet state and α-H transfers back to the higher energy $CH_2{=}MoH_2$ (S) singlet state, which is quenched to $CH_2{=}MoH_2$ (T) by the matrix. The latter is also excited to a higher triplet state some of which α-H transfers back to $CH_3{-}MoH$ (T) and is relaxed to the global minimum energy $CH_3{-}MoH$ (Q) species by the matrix. The relative energies of the ground and excited states involved are important, but the competing rates of relaxation and intersystem crossing also contribute to the relative photochemical product yields. It appears that matrix relaxation of the intermediate higher $CH_2{=}MoH_2$ triplet state to the ground $^3A''$ $CH_2{=}MoH_2$ state is faster than α-H transfer back to the excited $CH_3{-}MoH$ (T) state. Finally, it is clear that α-H transfer is a facile process among these energized molecules.

The group 4 metal−methane reaction systems gave the dimethyl metal dihydride secondary reaction product in spontaneous, exothermic reactions.[4−7] Our calculations find $(CH_3)_2$-MoH_2 to be a stable molecule, but the $CH_2{=}MoH_2 + CH_4$ reaction to form $(CH_3)_2MoH_2$ is exothermic by only 27 kcal/mol. The strong $Mo{-}H_2$ stretching frequencies are predicted 30−40 cm^{-1} higher than those for $CH_2{=}MoH_2$, and we have no significant evidence for another major reaction product in this spectral region.

Conclusions

Reaction of laser-ablated Mo atoms with CH_4 in excess argon forms the $CH_3{-}MoH$, $CH_2{=}MoH_2$, and $CH{\equiv}MoH_3$ molecules, which are identified from infrared spectra by isotopic substitution and density functional theory frequency calculations. B3LYP calculations, even with the approximations involved, accurately predict the Mo−H stretching frequencies and several important diagostic lower frequency modes involving carbon for the product molecules. These simple methyl, methylidene, and methylidyne molybdenum hydride molecules are reversibly interconverted by α-H transfers on excited quintet, triplet, and singlet electronic surfaces upon visible and ultraviolet irradiations. The methyl hydride CH_3MoH $^5A'$ state is the lowest energy product. The methylidene dihydride $CH_2{=}MoH_2$ $^3A''$ state exhibits distortion and agostic interaction to a lesser degree than $CH_2{=}ZrH_2$. The methylidyne trihydride $CH{\equiv}MoH_3$ is a stable $^1A_1$ state C_{3v} symmetry molecule, which is characterized through five observed vibrational frequencies.

Acknowledgment. We appreciate support from NSF Grant CHE 03-52487 to L.A.

Supporting Information Available: Complete ref 21. This material is available free of charge via the Internet at http://pubs.acs.org.

JA0511568

---

(32) Tsai, Y. C.; Diaconescu, P. L.; Cummins, C. C. *Organometallics* **2000**, *19*, 5260.

(33) Crabtree, R. H. *The Organometallic Chemistry of the Transition Metals*, Wiley: New York, 2001; p 190.

(34) It was difficult to optimize $CH_2{-}MoH_2$ (Q) because during the Gaussian geometry optimization reverse α-H transfer often gave the lower energy $CH_3{-}MoH$ (Q) product.

(35) Pellin, M. J.; Gruen, D. M.; Fisher, T.; Foosnaes, T. *J. Chem. Phys.* **1983**, *79*, 5871.